Development/Plasticity/Repair

ADAMTS4 Enhances Oligodendrocyte Differentiation and Remyelination by Cleaving NG2 Proteoglycan and Attenuating *PDGFRα* Signaling

Chunxia Jiang,[1,2] Wanwan Qiu,[2] Yingying Yang,[2] Hao Huang,[2] Zhong-min Dai,[2] Aifen Yang,[2] Tao Tang,[3] Xiaofeng Zhao,[2] and Mengsheng Qiu[1,2]

[1]College of Life Sciences, Zhejiang University, Hangzhou 310058, China, [2]Institute of Developmental and Regenerative Biology, Zhejiang Key Laboratory of Organ Development and Regeneration, College of Life and Environmental Sciences, Hangzhou Normal University, Hangzhou 310036, China, and [3]Department of Anatomy, Cell Biology and Physiology, Stark Neurosciences Research Institute, Indiana University School of Medicine, Indianapolis, Indiana 46202

Although NG2 is known to be selectively expressed in oligodendrocyte precursor cells (OPCs) for many years, its expressional regulation and functional involvement in oligodendrocyte differentiation have remained elusive. Here, we report that the surface-bound NG2 proteoglycan can physically bind to PDGF-AA and enhances PDGF receptor alpha (*PDGFRα*) activation of downstream signaling. During differentiation stage, NG2 protein is cleaved by A disintegrin and metalloproteinase with thrombospondin motifs type 4 (*Adamts4*), which is highly upregulated in differentiating OPCs but gradually downregulated in mature myelinating oligodendrocytes. Genetic ablation of *Adamts4* gene impedes NG2 proteolysis, leading to elevated PDGFRα signaling but impaired oligodendrocyte differentiation and axonal myelination in both sexes of mice. Moreover, *Adamts4* deficiency also lessens myelin repair in adult brain tissue following Lysophosphatidylcholine-induced demyelination. Thus, *Adamts4* could be a potential therapeutic target for enhancing oligodendrocyte differentiation and axonal remyelination in demyelinating diseases.

Key words: **Adamts4; differentiation; NG2; oligodendrocyte PDGFRa**

Significance Statement

NG2 is selectively expressed in OPCs and downregulated during differentiation stage. To date, the molecular mechanism underlying the progressive removal of NG2 surface proteoglycan in differentiating OPCs has been unknown. In this study, we demonstrate that ADAMTS4 released by differentiating OPCs cleaves surface NG2 proteoglycan, attenuates PDGFRα signaling, and accelerates oligodendrocyte differentiation. In addition, our study also suggests ADAMTS4 as a potential therapeutic target for promoting myelin recovery in demyelinating diseases.

Introduction

In the CNS, myelin sheaths are elaborated by oligodendrocytes (OLs), which originate from immature oligodendrocyte progenitor cells (OPCs). OPCs can be readily identified by their selective expression of two surface proteins, PDGF receptor alpha (PDGFRα) and NG2, a member of the chondroitin sulfate proteoglycan (CSPG4). Structurally, NG2 is an integral membrane protein with a large N-terminal extracellular domain, encompassing numerous glycosaminoglycan attachment sites (Larsen et al., 2003). *In vitro* studies based on the enzyme-linked immunosorbent assay and Biacore (biosensor system) assays showed that NG2 core protein can bind to PDGF A chain homodimer (PDGF-AA) with high affinity (Goretzki et al., 1999), although the direct evidence for their physical interaction is still lacking. Based on this observation, it has been postulated that NG2 may serve to enrich the local PDGF-AA concentration on the surface of OPCs and enhance *PDGFRα* signaling to stimulate OPC proliferation and maintain their progenitor state (Zhu et al., 2014). In NG2 null mutants, the number of both OPCs and myelinating oligodendrocytes is significantly diminished (Kucharova and Stallcup, 2010).

Received Nov. 19, 2022; revised May 3, 2023; accepted May 4, 2023.

Author contributions: C.J., H.H., Z.D., X.Z., and M.Q. designed research; C.J., W.Q., and Y.Y. performed research; C.J., W.Q., Y.Y., and A.Y. analyzed data; T.T. and M.Q. wrote the paper.

This work was supported by Ministry of Science and Technology China Brain Initiative Grant STI2030-Major Projects 2022ZD0204700, National Natural Sciences Foundation of China Grants 32070965 and 32170969, Natural Science Foundation of Zhejiang Province Grants LY22H090002 and LY22C090002, and Scientific Research Fund of Zhejiang Provincial Education Department Grant Y202147674.

The authors declare no competing financial interests.

Correspondence should be addressed to Mengsheng Qiu at m0qiu001@yahoo.com or Xiaofeng Zhao at xiaofengzhao@yahoo.com.

https://doi.org/10.1523/JNEUROSCI.2146-22.2023

During differentiation stage, expression of both *PDGFRα* and NG2 is downregulated in OPCs, with NG2 expression lasting slightly longer than *PDGFRα* (Nishiyama et al., 1996a). The downregulation of these molecular markers in differentiating OPCs appears to be necessary for their terminal differentiation and morphologic maturation, as continuous *PDGFRα* signaling represses OL differentiation (Zhu et al., 2014; Zhang et al., 2020), and extracellular CSPGs inhibit oligodendroglial process outgrowth and myelin elaboration (Siebert and Osterhout, 2011; Kuboyama et al., 2017). Although Nkx2.2-mediated transcriptional repression has been implicated in suppressing *PDGFRα* expression (Zhu et al., 2014), the molecular mechanism underlying the progressive removal of NG2 surface proteoglycan in differentiating OPCs has remained to be determined.

In the present study, we report that A disintegrin and metalloproteinase with thrombospondin motifs type 4 (*Adamts4*) is involved in the proteolytic cleavage of NG2 protein during oligodendrocyte differentiation. During early oligodendroglial development, *Adamts4* is markedly upregulated in differentiating oligodendrocytes and newly differentiated oligodendrocytes (NFOs) in the developing CNS. In both transfected cells and OPC primary culture, expression or inclusion of ADAMTS4 protease is capable of cleaving NG2 proteoglycan, which we found can physically interact with extracellular PDGFAA and enhance *PDGFRα* signaling. *Adamts4* null mutation slowed down NG2 proteolysis and enhanced ERK phosphorylation, leading to delayed oligodendrocyte differentiation in the forebrain. Furthermore, myelin recovery following Lysophosphatidylcholine (LPC)-induced demyelination is compromised in *Adamts4* mutants compared with wild-type mice.

Materials and Methods

Animals. B6.129P2-*Adamts4*^{tm1Dgen}/J mice with lacZ (bacterial β-galactosidase) reporter were obtained from The Jackson Laboratory (RRID:IMSR_JAX:005770). *Adamts4* mutant was generated and characterized by Deltagen through homologous recombination in embryonic stem cells. *Adamts4* KO is a global knockout and maintained on a C57BL/6J background. The *LacZ* gene was inserted into the exon 4 of *Adamts4* gene as a reporter, and its expression reflects that of the endogenous *Adamts4* gene. Mice expressing GFP under the control of the proteolipid protein promoter (*Plp*-eGFP) and oligodendrocyte lineage-specific reporter mouse (*Sox10*-GFP) were provided by Prof. Feng Yue and Prof. William D. Richardson, respectively (Mallon et al., 2002; Mallon and Macklin, 2002; Tripathi et al., 2011). *Adamts4* $^{-/-}$; *Plp*-eGFP mutants and *Adamts4* $^{-/-}$; *Sox10*-GFP mutants were produced by sequential breeding of *Adamts4* knock-out mice with *Plp*-eGFP and *Sox10*-GFP mice, respectively. PCR-genotyping was conducted using genomic DNA with the following primers: *Adamts4* knockout-p1(5′-GGG TGG GAT TAG ATA AAT GCC TGC TCT-3′), *Adamts4* knockout-p2 (5′-GGA CAC GGG ATG GAC CCT CTA GAT G-3′), *Adamts4* knockout-p3 (5′-ACA TGG AGG ACT CAG TGT GGC CCA C-3′); *Plp*-eGFP-p1 (5′-ACG TAA ACG GCC ACA AGT TC-3′), *Plp*-eGFP-p2 (5′-GGG GTG TTC TGC TGG TAG TG-3′); *Sox10*-GFP-p1 (5′-GCC ACG AGT TCG AGA TCG AG-3′), *Sox10*-GFP-p2 (5′-GGC TTC TTG GCC ATG TAG ATG G-3′). *Adamts4*-null allele resulted in a 495 bp band, whereas wild-type allele produced a 326 bp band, *Plp*-eGFP allele resulted in a 500 bp band, and *Sox10*-GFP allele resulted in a 465 bp band. Animals of either sex were used for analyses. All experiments were conducted in accordance with the Institutional Animal Care and Use Committee of Hangzhou Nomal University.

Cell culture. HEK 293T cells were cultured in DMEM medium containing 10% FBS. Plasmids were introduced into cells with Lenti-Pac Kit (catalog #BK-AC00, Oasis Biofarm), and fresh medium was added at 12 h after transfection. For transfection, ORF of *Adamts4* [accession #NM_172845.3, National Center for Biotechnology Information (NCBI)] and *NG2* (accession #NM_139001.2, NCBI) were inserted after the CMV promoter or EF1 promoter in *pCDH* vectors (catalog #CD511B-1, System Biosciences). Tags fused with ADAMTS4 and NG2 are as diagrammed in the figures. For coimmunoprecipitation assays, *Myc* in *pCDH-EF1-NG2-Myc* vectors was replaced by *Flag*.

Primary OPCs were purified from postnatal day 1 (P1) Sprague Dawley rats or *Adamts4* mutant pups as described previously (Chen et al., 2015; Jiang et al., 2018). rhADAMTS4 protein (catalog #4307-AD-020, R&D Systems) was added to the medium at 24 h after OPCs plated. Ninety-six hours after treatment, cells were collected for Western blot or immunofluorescent staining.

In situ hybridization and immunofluorescence staining

Mice were anesthetized, and CNS tissues were isolated and fixed in 4% paraformaldehyde (PFA) at 4°C overnight, then transferred into 25% sucrose for equilibration. Tissues were embedded in OCT and cryosectioned into 16-μm-thick sections. For *in situ* hybridization (ISH), *Adamts4* riboprobe corresponding to 314–1341 nt of mouse *Adamts4* mRNA (accession #NM_172845.3, NCBI) was generated *in vitro* from the cDNA template subcloned into pBluescript II KS^{+} vector. Experimental procedures for ISH were described previously (Zhu et al., 2013). For immunofluorescence, sections or cells were permeabilized with PBS 5 min for three times and blocked in PBS containing 5% goat serum and 0.1% Triton X-100 for 30 min at 37°C. For bromodeoxyuridine (BrdU) immunostaining, sections or cells were incubated in 2N HCl for 20 min at room temperature to denature DNA before blocking. Sections or cells were then incubated with primary antibody at 4°C overnight as follows: anti-β-Gal (1:300; catalog #Z378A, Progema), anti-NG2 (1:1000; catalog #AB5320, Millipore; RRID: AB_11213678), anti-NG2 (1:400; catalog #OB-PGP002, Oasis Biofarm), anti-SOX10 (1:500; catalog #OB-PGP001, Oasis Biofarm; RRID: AB_2934230 and 1:500, catalog #OB-PRB053, Oasis Biofarm; AB_2934229), anti-CC1 (1:500; catalog #OB-PRB070, Oasis Biofarm; RRID: AB_2934254 and #OB-PRT039, Oasis Biofarm; RRID: AB_2938673 Oasis Biofarm), anti-MYRF (1:500; catalog #OB-PRT003, Oasis Biofarm; RRID: AB_2938674 and # OB-RB007, Oasis Biofarm; RRID: AB_2934225), anti-ASPA (1:500; catalog #OB-PRT005, Oasis Biofarm; RRID: AB_2938679 and 1:500, #OB-RB037, Oasis Biofarm, Oasis Biofarm; RRID: AB_2938680), anti-BrdU (1:500; catalog #OB-MMS018, Oasis Biofarm; RRID: AB_2938682). On the next day, the secondary antibodies were applied at room temperature for 1 h. Secondary antibodies included goat anti-rabbit IgG (H + L; 1:3000; catalog #A11012 and #A11034, Invitrogen), Goat anti Mouse IgG1(1:3000; catalog #A21125 and #A21121, Invitrogen), goat anti-rat IgG (H + L; 1:3000; catalog #A11007 and #A11006, Invitrogen) and goat anti-mouse IgG (1:2000; catalog #76085, Sigma-Aldrich). Tissues or cells were then washed 5 min for three times in PBS and mounted with Mowiol mounting medium for fluorescence microscope observations.

Western blotting. Tissues were lysed in RIPA lysis buffer (catalog #P0013B, Beyotime) with Protease Inhibitor Cocktail (catalog #P8340, Sigma-Aldrich). Protein concentration was measured by bicinchoninic acid protein assay kit (catalog #23225, Thermo Fisher Scientific). The total protein was subjected to electrophoresis in 10% SDS-PAGE gel and then transferred to PVDF membrane. The membrane was blocked with 5% nonfat milk at room temperature for 1 h and then incubated with primary antibody at 4°C overnight. The sources and dilutions of primary antibodies are as follows: anti-β-actin (1:10,000; catalog #AC026, ABclonal), anti-GAPDH (1:10,000; catalog #ABS16, Millipore; RRID: AB_11211543), anti-MYC (1:1000; catalog #2276, Cell Signaling Technology; RRID:AB_331783), anti-NG2 (1:1000; catalog #AB5320, Millipore; RRID:AB_11213678), anti-PDGFR-α (1:100; catalog #sc-338, Santa Cruz Biotechnology; RRID:AB_631064), anti-PDGFR-α (1:1000; catalog #OB-PRB011, Oasis Biofarm; RRID: AB_2938683), anti-ERK1/2 (1:5000; catalog #A16686, ABclonal), and anti-Phospho-ERK1/2 (1:000; catalog #ab229912, Abcam). GAPDH or β-actin was used as an internal control. On the next day, the membrane was washed 10 min for three times in TBST and incubated with a secondary antibody conjugated to HRP for ECL detection.

Immunoprecipitation. HEK293T cells were transfected with pCDH-*PDGF-A*-3×HA (Huang et al., 2017) or/and pCDH-NG2-3×Flag vector.

After 48 h, HEK293T cells in each 3.5 cm dish were washed with PBS and lysed in 1 ml of lysis buffer containing 25 mM Tris, pH 7.4, 150 mM NaCl, 1% NP40, 0.25% sodium deoxycholate, and protease inhibitor cocktail (Sangon Biotech) at 4°C for 5 min; 0.2 ml of lysate was used as the input sample. For FLAG-tagged proteins, 20 µl of anti-FLAG magnetic beads (catalog #M8823, Sigma-Aldrich) was added into the left lysate at 4°C overnight. Beads were then washed with lysis buffer, and the FLAG-tagged protein was eluted with 200 µl lysis buffer containing 7.5 µg 3 × Flag peptides per sample. For HA-tagged proteins, 200 µl of anti-HA magnetic beads (catalog #M8823, Sigma-Aldrich) was added into the remaining lysate and incubated at room temperature for 30 min with mixing. Beads were washed 5 min for three times with TBST, and 200 µl of Sample Buffer was added to the tube and incubated at 98°C for 5 min. Beads were separated magnetically, and the supernatant containing the target antigen was collected. Both input and IP samples were subjected to Western blot with anti-FLAG (1:1000; catalog #F1804, Sigma-Aldrich; RRID: AB_262044) and anti-HA (1:5000; catalog #H3663, Sigma-Aldrich; RRID:AB_262051).

Fluorescent assay of ADAMTS4 activity. ADAMTS4 is also known as Aggrecanse-1 because it can cleave Aggrecan in cartilage (Tortorella et al., 1999). To measure ADAMTS4 activity, we used the SensoLyte 520 Aggrecanase-1 Fluorometric Assay Kit (catalog #AS-72114, AnaSpec). Briefly, 50 µl of conditional medium from transfected HEK293T cells and 50 µl of aggrecanase substrate solution were added into a 96-well black plate (catalog #26019004, Corning) and then incubated for 30 min at 37°C. Fluorescence was measured using a fluorescence microplate reader (Tecan Spark 10M) equipped with a 490 nM excitation filter and a 520 nM emission filter. Concentrations of ADAMTS4 were calculated according to the reference standard curve.

Cell proliferation assay. Two hundred microliters of 10 mg/ml BrdU (catalog #B5002, Sigma-Aldrich) were administered to P15 mice via intraperitoneal injection 2 h before tissue collection. Brain tissues were then fixed and sectioned for histochemical analyses as described above. For OPC proliferation assays in primary culture, 10 µM BrdU was added to medium 4 h before immunofluorescence staining was performed.

Gold myelin staining kit. Frozen sections were prepared at 18 µm thickness and rehydrated in ddH_2O for 2 min, then transferred to prewarmed Gold myelin staining solution (catalog #BK-AC001, Oasis Biofarm) and incubated in a 45°C hybridization oven until the finest myelinated fibers emerged. The sections were rinsed two times in ddH_2O for 2 min each. Sodium thiosulfate solution was added and incubated at 45°C for 3 min. The sections were then rinsed three times in ddH_2O for 2 min each and coverslipped with Mowiol mounting medium for bright field microscope observations.

Focal demyelination procedure. Two microliters of 1% LPC (catalog #L1381, Sigma-Aldrich) was injected slowly (0.075 µl/min) into corpus callosum (AP, +0.10 mm; ML, −0.14 mm; DV, −0.20 mm relative to bregma) of 8-week-old mice as described previously (Nait-Oumesmar et al., 1999). Mice were allowed to recover and were killed at 7, 14, and 21 d postinjury (dpi). Brain tissues were then fixed and sectioned for histochemical analyses.

Experimental design and statistical analyses. For statistical analysis, at least three representative images of brain sections from comparable positions were acquired for each group. Quantification was performed using ImageJ software version 2.9.0 (National Institutes of Health). The data were analyzed by two-tailed Student's *t* test, and *p* values <0.05 were considered to be statistically significant ($n \geq 3$). Error bars indicate SEM.

Results

Adamts4 is selectively upregulated in differentiating oligodendrocytes in the CNS

NG2 surface proteoglycan is abundantly expressed in OPCs but gradually fades away as they undergo terminal differentiation. To determine which metalloproteinases are likely to be involved in the progressive removal of the NG2 protein, we first examined the expression of several important metalloproteinases of the ADAMTs family by ISH in P15 cortical tissue of *Sox10*-GFP transgenic mice. Among the six members investigated, only *Adamts4* was found to be coexpressed in *Sox10*-GFP$^+$ oligodendrocytes (Fig. 1*A*,*B*). Detailed spatiotemporal expression of *Adamts4* was analyzed in the B6.129P2-*Adamts4*$^{tm1Dgen/J}$ mouse line, in which the LacZ reporter gene is knocked into the *Adamts4* locus and thus represents the endogenous *Adamts4* expression (Fig. 1*C*). Double immunostaining in postnatal *Adamts4*$^{+/-}$; *Sox10*-GFP double heterozygous reporter mice demonstrated that nearly all *LacZ*$^+$ cells in the corpus callosum were immunoreactive to *Sox10*-GFP (Fig. 1*D1*,*E*), suggesting that *Adamts4* is primarily expressed in cells of oligodendrocyte lineage. Consistently, *Adamts4*-LacZ staining was specifically detected in MYRF- and CC1-expressing oligodendrocytes in postnatal corpus callosum (Fig. 1*D2*,*3*,*E*). However, *Adamts4* expression was barely observed in *Pdgfrα*$^+$ OPCs (Fig. 1*F*,*G*) and markedly downregulated in ASPA$^+$ myelinating OLs (Huang et al., 2023) (Fig. 1*H*,*I*), suggesting that it is primarily expressed in differentiating OPCs and NFOs. This concept was further verified by the remarkable reduction of *Adamts4* expression in the white matter of P3 spinal cord of *CNP*$^{Cre/+}$; *Nkx2.2*$^{flox/flox}$ mice (Fig. 1*J*,*K*). *Nkx2.2* mutation was shown to cause a severe delay of OL differentiation at early postnatal stage (Qi et al., 2001; Zhu et al., 2014). Together, these findings establish that *Adamts4* is selectively upregulated in oligodendrocyte lineage during the differentiation stage.

ADAMTS4 expression is associated with increased cleavage of NG2 surface protein on OPCs

Previous studies suggested that ADAMTs function to digest extracellular matrix and proteoglycans (Lemarchant et al., 2013). Noticeably, as *Adamts4* expression is progressively elevated in oligodendrocyte lineage during the differentiation stage (Fig. 2*A*, *B*), the intensity of NG2 immunostaining gradually fades away. This inverse relationship prompted us to hypothesize that NG2 proteoglycan is a direct target of ADAMTS4 proteinase. To test this hypothesis, we transfected HEK 293T cells with NG2-myc expressing construct alone or in conjunction with the *Adamts4*-flag expressing vector. For NG2-myc transfection alone, the transfected cells displayed a strong NG2 immunofluorescent signal on the cell surface (Fig. 2*C1–3*,*D*). In ADAMTS4-Flag coexpressed cells, NG2 staining was significantly reduced (Fig. 2*C4–6*,*D*). Western immunoblotting with either anti-NG2 or anti-MYC antibody detected a single protein band of ~280 kDa in NG2-myc transfected cells. In the cotransfected cells, a new 150 kDa species emerged in parallel to the diminished intensity of the 280 kDa band (Fig. 2*E*). To further test the idea that NG2 protein can be directly cleaved by ADAMTS4, we treated OPC primary culture with recombinant human ADAMTS4 protein and discovered that this treatment produced two protein bands corresponding to the truncated 150 kDa and the full-length 280 kDa proteins, whereas the untreated OPCs only yielded the 280 kDa species (Fig. 2*F*). In addition, OPCs were purified from WT and *Adamts4* mutant brain tissues and differentiated *in vitro* for 2 d (2 DIV) in differentiation medium. Immunostaining revealed that the full-length NG2 protein was markedly reduced in control OPCs after 2 DIV, and the 150 kDa fragment was only evident in control cells but not in mutant cells (Fig. 2*G*). Collectively, these results provided strong evidence that oligodendrocytes undergo an autonomous regulation of NG2 cleavage mediated by increased expression of ADAMTS4 protease during the differentiation phase.

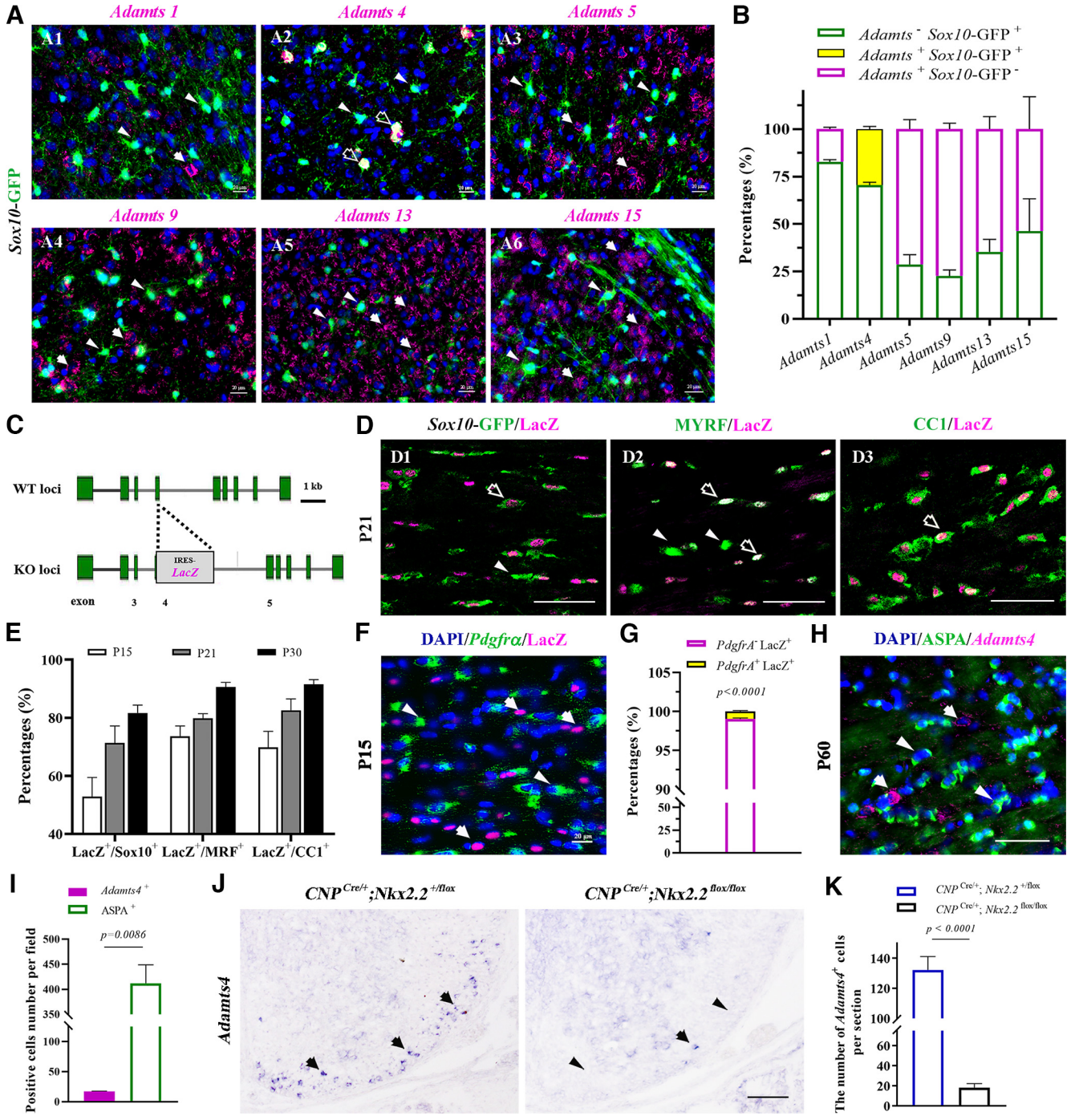

Figure 1. *Adamts4* is upregulated in premyelinating OLs in the corpus callosum. ***A1–6***, Expression of *Adamts* 1, 4, 5, 9, 13, and 15 were examined in P15 *Sox10*-GFP mouse cortex by ISH, and only *Adamts*4 was expressed in oligodendrocytes. *Sox10*$^+$ oligodendrocytes were tagged with GFP, and ADAMTSs mRNA signals were magenta. Arrowheads indicate *Sox10*-GFP$^+$ oligodendrocytes, arrows indicate mRNA signals of various *Adamts* genes, and open arrows indicate *Adamts4*$^+$*Sox10*-GFP$^+$ cells. Scale bar, 20 μm. ***B***, Statistical analysis of the percentage of *Adamts*$^-$ *Sox10*-GFP$^+$, *Adamts*$^+$ *Sox10*-GFP$^+$, and *Adamts*$^+$ *Sox10*-GFP$^-$ cells relative to the total in corpus callosum sections at P15; $n \geq 3$. ***C***, Schematic illustration of the construction strategy for the B6.129P2-*Adamts4*$^{tm1Dgen/J}$ knock-in mice. A Lac0-SA-IRES-*LacZ*-Neo555G/Kan cassette is inserted into the *Adamts4* gene to replace the exon 4. ***D1–3***, Representative images showing the coimmunostaining of lacZ (magenta) with various stage-specific oligodendrocyte markers (green) in P21 corpus callosum. LacZ-positive oligodendrocytes are represented by arrows and LacZ-negative cells by arrowheads. Scale bar, 50 μm. ***E***, Statistical analysis of the percentage of LacZ$^+$ cells in *Sox10*-GFP$^+$, MYRF$^+$, and CC1$^+$ populations in corpus callosum sections from P15 to P30; $n = 3$. ***F***, Brain tissues from P15 *Adamts4*$^{+/-}$ mice were subjected to ISH with *Pdgfrα* riboprobe (green), followed by LacZ immunofluorescent staining (magenta). *Pdgfrα*$^+$ OPCs are represented by arrowheads. Scale bar, 20 μm. ***G***, Statistical analysis of the percentage of *Pdgfrα*$^+$ OPCs in LacZ$^+$ cells in P15 callosal tissues; $n = 3$. ***H***, Brain tissues from P60 wild-type mice were subjected to ISH with *Adamts4* riboprobe (magenta), followed by immunofluorescent staining with anti-ASPA (green). Scale bar, 20 μm. ***I***, Statistical analysis of the number of ASPA$^+$ and *Adamts4*$^+$ cells per field in P60 corpus callosum; $n = 3$. ***J***, ISH showing the dramatic reduction of *Adamts4*$^+$ cells in P3 *Nkx2.2* CKO mouse spinal cord. Only the ventromedial regions of the spinal cords are shown. Arrows indicate Adamts4 mRNA signals. Scale bar, 100 μm. ***K***, Statistical analysis of the number of *Adamts4*$^+$ cells per section at P3; $n = 3$.

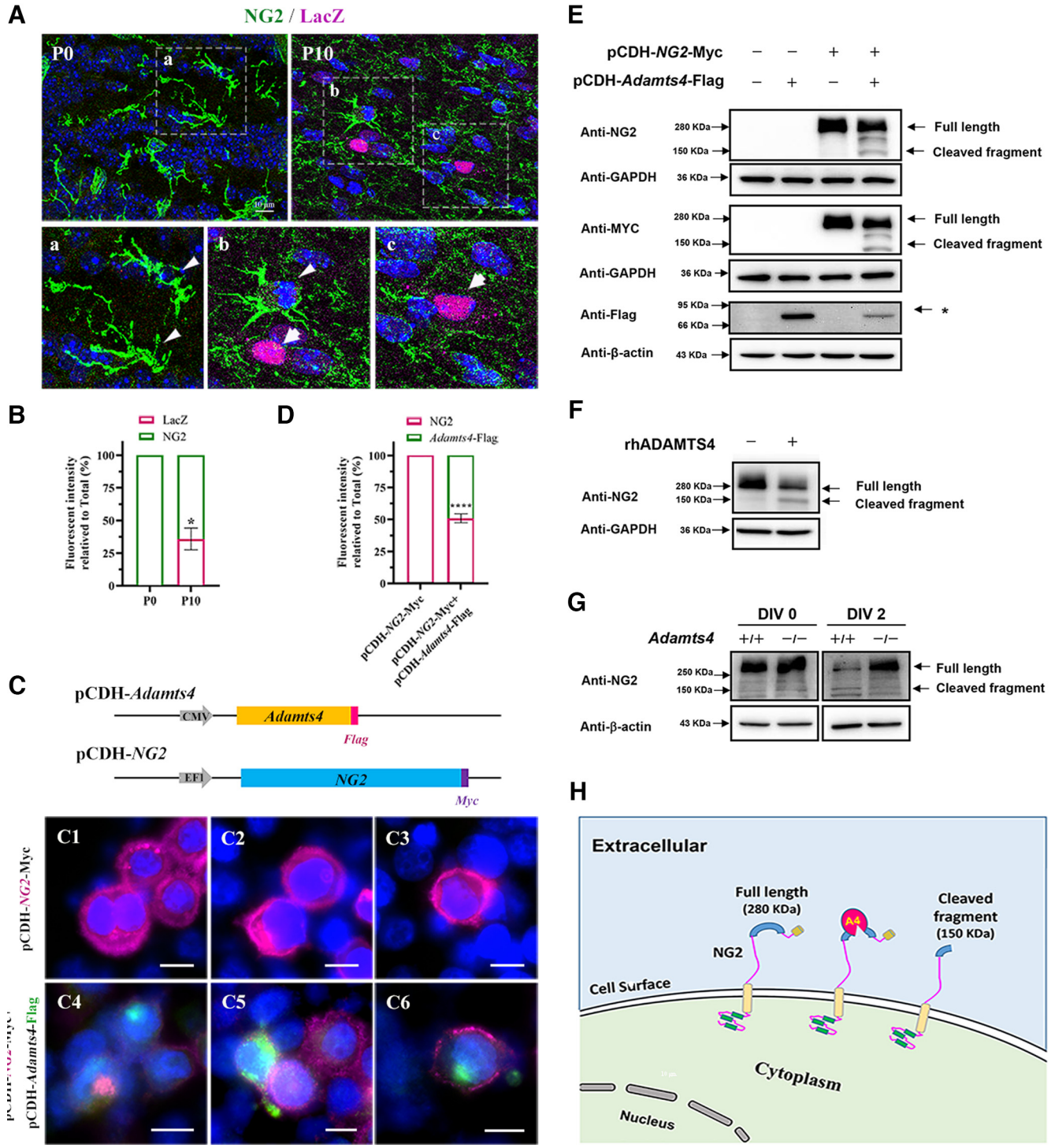

Figure 2. Proteolytic cleavage of NG2 protein by ADAMTS4. ***Aa–c***, Immunofluorescent staining for NG2 (green) and LacZ (magenta) in the corpus callosum of heterozygous mice at P0 and P10. Scale bar, 10 μm. ***B***, Statistical analysis of the fluorescent intensity of LacZ and NG2 per field. At least three representative fields were used from each brain section; $n = 3$; $^{*}p = 0.0122$. ***C***, A schematic diagram of the pCDH-*Adamts4*-Flag and pCDH-*NG2*-Myc expression constructs. ***C1–6***. Immunofluorescent staining of transfected HEK 293T cells with anti-NG2 (magenta) and anti-Flag (green) antibodies. Cells were transfected with indicated constructs for 48 h. Scale bar, 10 μm. ***D***, Statistical analysis of the fluorescent intensity of LacZ and NG2 per field. At least three fields were randomly acquired from each group; $n = 3$; $^{****}p < 0.0001$. ***E***, Western blot with HEK 293T cells at 48 h after transfection. (* represents the Adamts4-Flag protein. ***F***, Western blotting with primary OPC culture treated with rhADMATS4 proteinase. ***G***, Western immunoblot for detection of NG2 expression in primary culture of OPCs isolated from WT and *Adamts4* knockout mice. OPCs were cultured in differentiation medium for 0 and 2 d. ***H***, Schematic illustration of ADAMTS4 cleaving NG2 protein.

ADAMTS4 attenuates PDGFR-A stimulation of Erk phosphorylation

Previous studies suggested that the NG2 core protein contains several binding sites for PDGF-AA (Nishiyama et al., 1996b; Goretzki et al., 1999). However, there is a lack of experimental evidence for their physical interactions. To address this issue, we cotransfected HEK293T cells with pCDH-*PDGFA*-3×HA and pCDH-*NG2*-Flag, followed by coimmunoprecipitation experiments. We found that the NG2 protein indeed can be immunoprecipitated with the PDGF-A protein (Fig. 3*B*,*C*). As

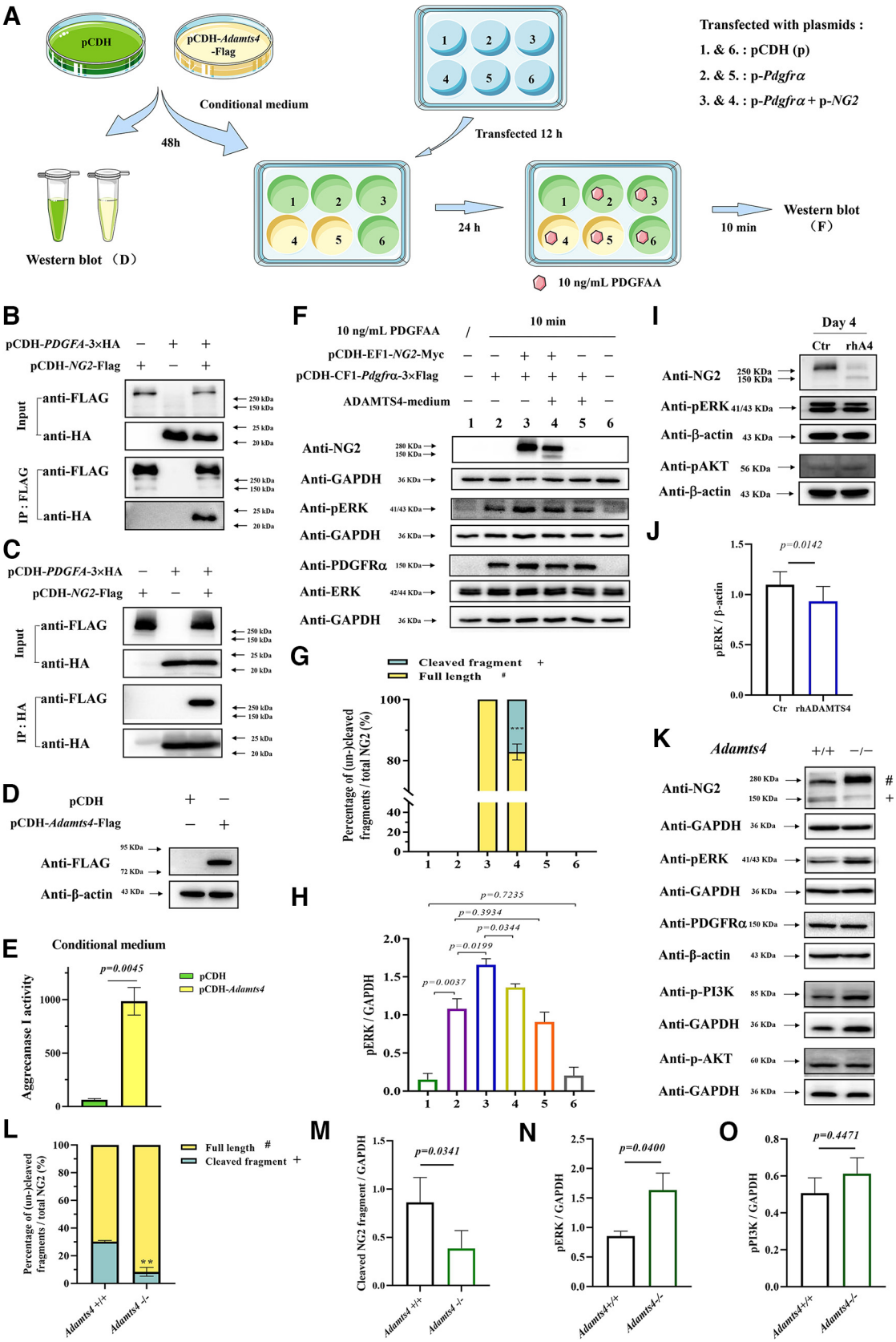

Figure 3. Effects of ADAMTS4 expression on NG2 proteolysis and PDGFRα-induced Erk signaling. ***A***, A diagrammatic illustration of experimental procedure. ***B***, ***C***, Physical interactions between PDGF-A and NG2 proteins. ***D***, Detection of ADAMTS4-Flag protein in lysed cells by Western blot 48 h after HEK293T cells were transfected with pCDH vector (control group) or pCDH-*Adamts4*-Flag construction (experimental group). ***E***, Detection of ADAMTS4 proteinase (Aggrecanase I) activity in HEK293T cells transfected with pCDH vector (control group) or pCDH-*Adamts4*-Flag construction (experimental group). Only supernatants were analyzed with the SensoLyte 520 Aggrecanase-1 Assay Kit (catalog #AS-72114, AnaSpec). ***F***, HEK293T cells were transfected with pCDH empty vector (wells 1 and 6), pCDH-CF1-*Pdgfrα*—3×Flag plasmid alone (wells 2 and 5) or together with pCDH-NG2-Myc plasmid (wells 3 and 4). After 12 h, wells 1, 2, 3, and 6

we showed that NG2 can be cleaved by ADAMTS4 protease, we reasoned that elevated ADAMTS4 expression would mitigate PDGF-AA activation of PDGFRα signaling. To test this idea, we first collected the conditioned medium from *Adamts4*-transfected HEK293T cells (Fig. 3*A*). Western blot and aggrecanase-1 assays confirmed that the ADAMTS4 protein was expressed and secreted into the culture medium (Fig. 3*D*,*E*). In a separate experiment, HEK293T cells were transfected with pCDH-CF1-*Pdgfrα*−3×Flag construct alone or together with pCDH-NG2-Myc construct, and Western blot analysis verified the expression of PDGFRα protein in both groups (Fig. 3*F*). Transfected cells were then treated with control or ADAMTS4-containing conditioned medium for 24 h, followed by the addition of 10 ng/ml PDGF-AA for 10 min. As expected, the level of phosphorylated ERK (pERK) increased remarkably in the PDGFRα-expressing group after PDGF-AA stimulation and was further elevated in cells that coexpressed pCDH-NG2-Myc (Fig. 3*F*,*H*). Treatment with ADAMTS4 conditioned medium significantly abated the level of NG2 protein and the intensity of pErk signal simultaneously in the cotransfected cells (Fig. 3*F–H*). Similarly, treatment of OPC primary culture with recombinant human ADAMTS4 protein also led to a small decrease of ERK phosphorylation (Fig. 3*I*,*J*). Noticeably, it had little or no effect on the level of pAKT (phosphorylated protein kinase B; Fig. 3*I*). Therefore, the presence of ADAMTS4 indeed attenuated the NG2-enhanced PDGF-AA activation of ERK phosphorylation.

Next, we examined whether the *Adamts4*-mediated cleavage of the NG2 protein also occurs during *in vivo* development of oligodendrocyte lineage. Western blot with P21 normal corpus callosum tissue detected both the full-length and cleaved NG2 protein bands (Fig. 3*K*,*L*), similar to those observed in transfected cells. However, in the *Adamts4*-KO mice, the ratio of the cleaved fragment to that of full-length protein was dramatically lowered (Fig. 3*K–M*). In parallel to the diminished NG2 degradation, the pERK signal was upregulated despite the unaltered PDGFRα protein level in the mutant tissue (Fig. 3*K*,*N*). In addition, the p-PI3k was slightly but insignificantly increased in the mutants, whereas the pAKT signal was unaltered (Fig. 3*K*,*O*). These results provided *in vivo* evidence that ADAMTS4-assisted NG2 degradation indeed occurs during OL development to help extinguish *PDGFRα* signaling and facilitate OL differentiation.

Oligodendrocyte differentiation and developmental myelination are impaired in *Adamts4* mutants

The selective upregulation of *Adamts4* expression in differentiating OPCs and NFOs has suggested its important role in regulating the differentiation and maturation of OLs. To test this possibility, we first examined the expression of mature OL marker myelin proteolipid protein (PLP) in the *Adamts4*$^{-/-}$*Plp*-eGFP mice (Fig. 4*A*). We found that the level of *Plp*-eGFP expression in the corpus callosum was significantly reduced in the *Adamts4*$^{-/-}$ mutant background at P15–P30 (Fig. 4*C*,*D*,*K*). Similarly, the expression of CC1, a marker for both NFO and differentiated OLs, was also diminished in the corpus callosum of *Adamts4*$^{-/-}$ mice (Fig. 4*E*,*F*,*L*). In addition, the number of ASPA$^+$ cells, which represent more mature myelinating OLs (Bhakoo et al., 2001; Mattan et al., 2010; Huang et al., 2023), also declined in the corpus callosum of the mutants (Fig. 4*G*,*H*,*M*). However, the number of *Sox10*-GFP$^+$ cells in the corpus callosum was similar between the mutants and their control littermates, indicating that the total number of oligodendrocytes was not altered by *Adamts4* mutation (Fig. 4*B*,*I*,*J*,*N*). Cell proliferation assays in P15 corpus callosum revealed that deficiency of *Adamts4* led to a slight increase of BrdU$^+$/Sox10$^+$ OPCs and *Pdgfrα*$^+$ OPCs in mutant tissue (Fig. 4*O–T*), in association with the compromised differentiation. Together, these findings suggested that *Adamts4* mutation mainly affected oligodendrocyte differentiation and maturation with only a mild effect on OPC proliferation. However, when OPCs were cultured with recombinant human ADAMTS4 protein in the presence of PDGF AA (Fig. 4*U*,*V*), the percentage of BrdU-positive cells in SOX10$^+$ oligodendrocyte population was significantly reduced, indicating that ADAMTS4 had a larger effect on slowing down OPC proliferation *in vitro* (Fig. 4*W*).

The hindered oligodendrocyte differentiation in the absence of *Adamts4* expression prompted us to study how myelin development was affected in the mutants. It was found that in *Adamts4* $^{-/-}$; *Plp*-eGFP mice, the number of GFP$^+$ oligodendrocytes and their associated myelin fibers was significantly reduced in the retrosplenial dysgranular cortex and adjacent cortical regions in P15 mutants (Fig. 5*A–H*). This result was further substantiated by Gold myelin staining, which revealed a remarkable reduction of myelin fibers in the cortical plate and the underlying corpus callosum in the knock-out mice (Fig. 5*I–P*). Together, these molecular and morphologic analyses provide a strong argument that *Adamts4* possesses an important role in regulating oligodendrocyte differentiation and myelination in the developing brain.

Myelin regeneration is impaired in the *Adamts4* null mutants

As *Adamts4* deletion has a significant impact on oligodendrocyte differentiation and early myelinogenesis, we next investigated the role of *Adamts4* in myelin repair after injury. Axonal demyelination was induced in corpus callosum by lysolecithin injection (Fig. 6*A*). At 7 dpi, we observed that *Adamts4* mRNA expression was markedly upregulated in the LPC-injected area (Fig. 6*C2*,*D*) but gradually decreased during the remyelination phase and returned to the undetectable level at the end of remyelination (Fig. 6*C3*,*D*). Immunofluorescent staining confirmed the selective upregulation of *Adamts4* expression in SOX10$^+$ oligodendrocytes during the remyelination period (Fig. 7). The initial injured areas induced by LPC injections were similar between the wild-type and *Adamts4* deficient mice (Fig. 6*E1*,*E2*,*E7*). However, at 14 and 21 dpi, the MBP-negative unmyelinated area in *Adamts4* null mice was significantly and consistently larger than that in the wild-type mice (Fig. 6*E3–6*,*E7*). Meanwhile, the density of CC1$^+$ and ASPA$^+$ cells in the injured areas was also significantly lower in the mutants (Fig. 6*F*,*G*). Axonal remyelination

←

were cultured in control conditioned medium, whereas wells 4 and 5 were replaced with conditioned medium containing ADAMTS4 protease. At 36 h after transfection, 10 ng/ml PDGFAA was added to wells 2–6. After 10 min, cells were harvested for Western blot analysis with specific antibodies. ***G***, Ratio of the cleaved NG2 fragment to the full-length NG2 protein in transfected HEK293T cells ($n = 3$, ***$p = 0.0002$). ***H***, The relative ratio of pERK to GAPDH in transfected HEK293T cells ($n = 3$). ***I***, Western immunoblot for detection of NG2, pAKT, and pERK expression in primary rat OPC culture treated with PDGFAA for 3 d in the presence or absence of rhADAMTS4 proteinase. PDGFA was withdrawn for 1 d before it was added back for 15 min. ***J***, Quantifications of pERK expression in primary rat OPC culture ($n \geq 3$). ***K***, Western immunoblot for detection of NG2, pERK, PDGFRα, p-PI3K, and pAKT expression in P21 corpus collosum of *Adamts4*-KO mice; (# and + represent the full-length and cleaved fragment of NG2 proteins, respectively). ***L***, Ratio of the cleaved NG2 protein relative to the full-length NG2 protein in P21 corpus callosum ($n = 3$, **$p = 0.0028$). ***M–O***, Quantifications of cleaved NG2 fragment, pERK, and p-PI3K in P21 corpus callosum ($n = 3$).

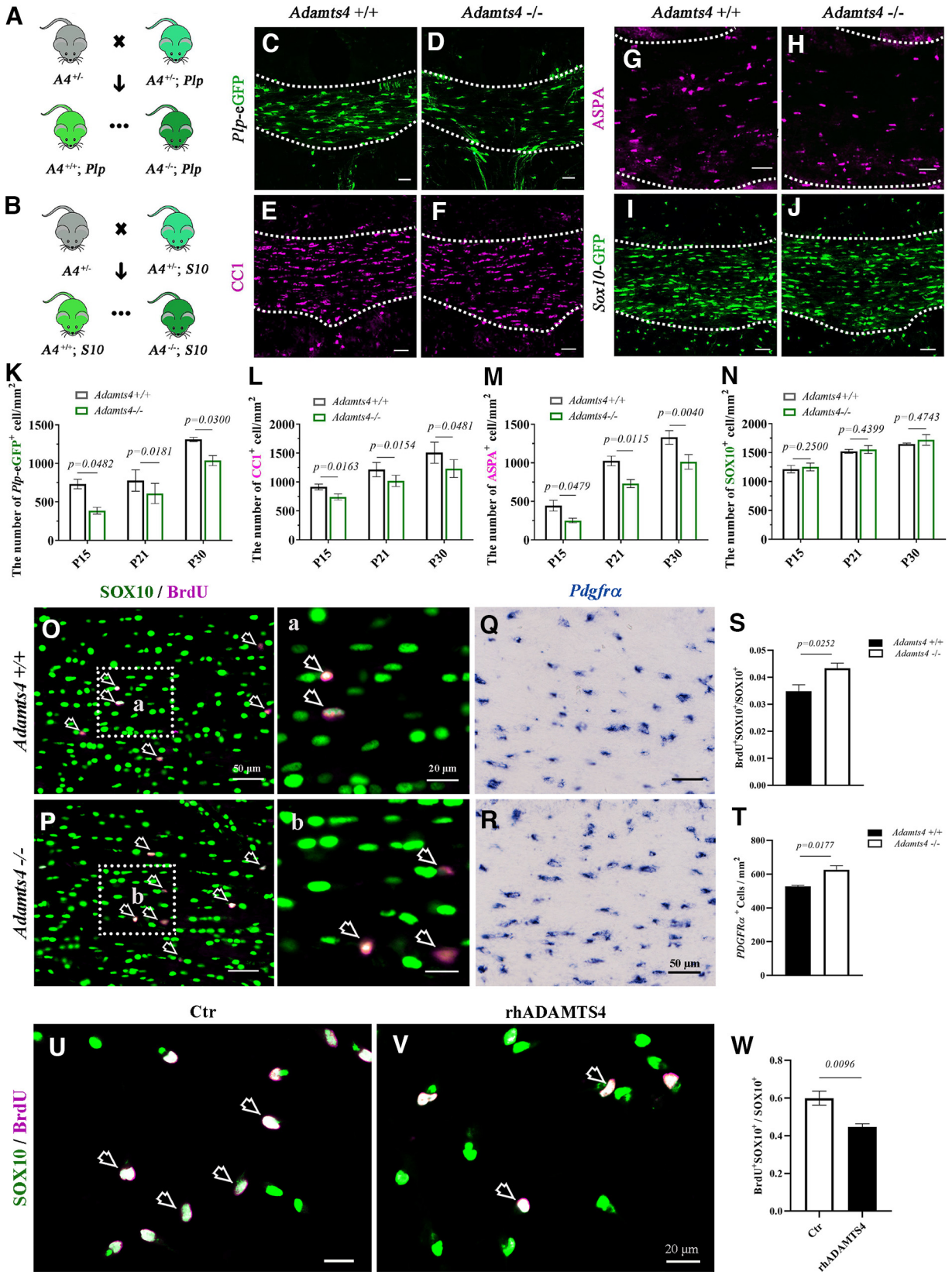

Figure 4. Impaired oligodendrocyte differentiation in *Adamts4* mutants. ***A***, ***B***, Strategy for generating of *Adamts4* $^{-/-}$; *plp*-eGFP mutants (***A***) and *Adamts4* $^{-/-}$; *Sox10*-GFP mutants (***B***). *A4*, *Adamts4*; *Plp*, *Plp*-eGFP; *S10*, *Sox10*-GFP. ***C***, ***D***, The number of *Plp*-eGFP^{+} oligodendrocytes decreased in the corpus callosum of *Adamts4* null mice. ***E–H***, Immunofluorescent staining of anti-CC1 and anti-ASPA in the corpus callosum of *Adamts4* knock-out mice. Scale bar, 50 μm. ***I***, ***J***, Comparable number of *Sox10*-GFP^{+} cells in the corpus callosum of WT and *Adamts4*$^{-/-}$ mice. ***K–N***, Statistical analysis of the number of *Plp*-eGFP^{+}, CC1^{+}, ASPA^{+}, and *Sox10*-GFP^{+} oligodendrocytes per square millimeter in corpus callosum sections; $n = 3$; p values are shown on the bar graphs. ***O***, ***Oa***, ***P***, ***Pb***, Coimmunofluorescence staining in P15 corpus callosum showed a slight increase of the ratio of BrdU^{+} dividing cells (magenta) in SOX10^{+} oligodendrocytes (green) in *Adamts4* mutants. Scale bar, 50 μm. Higher-magnification images are shown in ***a***, ***b***. Scale bar, 20 μm. Open arrows, BrdU^{+} SOX10^{+} cells. ***Q***, ***R***, *In situ* RNA hybridization revealed a slight increase of *Pdgfrα*$^{+}$ OPCs in P15 corpus callosum of *Adamts4* mutants; $n = 3$. Scale bar, 50 μm. ***S***, Statistical analysis of the number of BrdU^{+} cells in SOX10^{+} oligodendrocytes in corpus

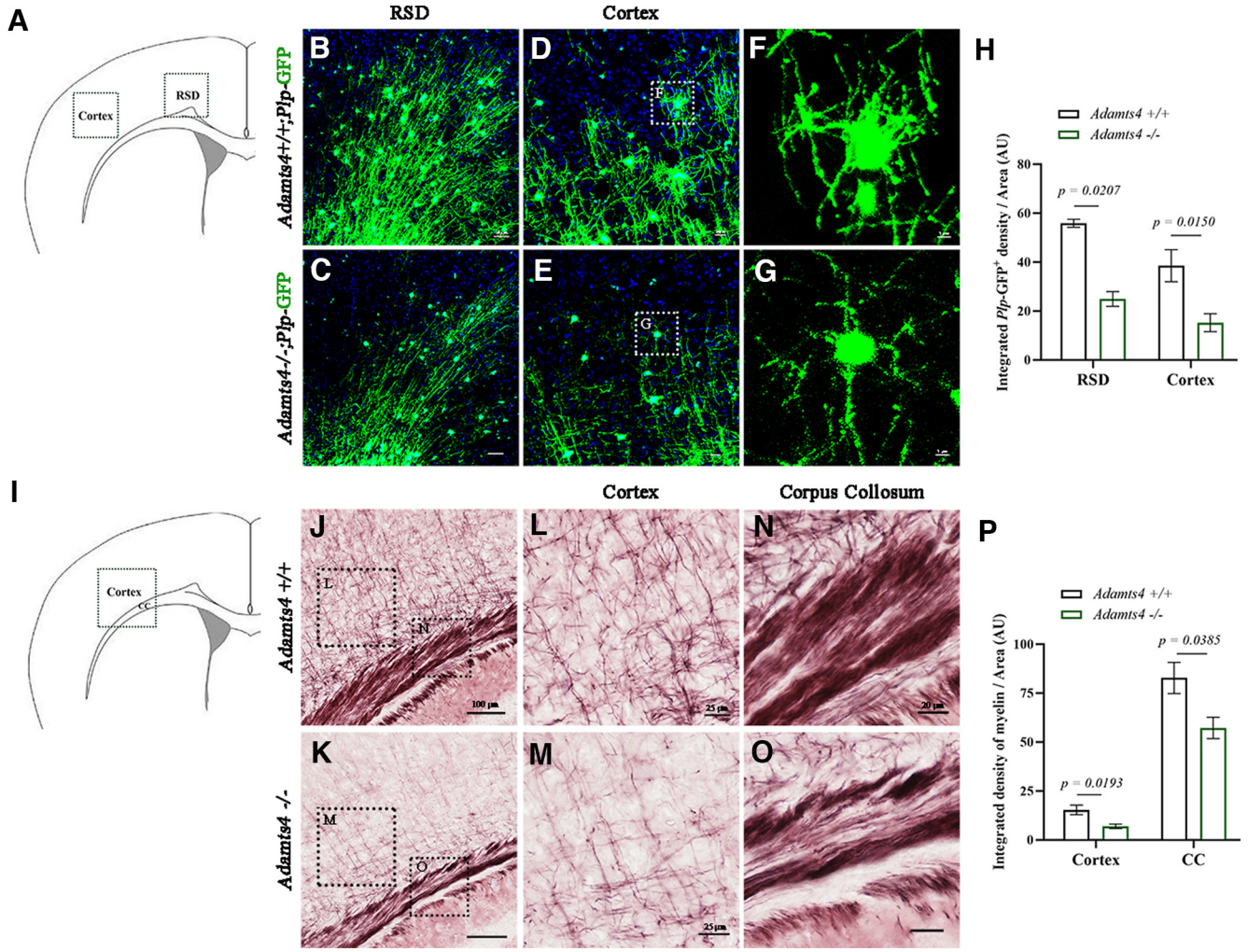

Figure 5. Defective developmental myelination in the cortex of *Adamts4* mutants. ***A–G***, Immunofluorescence of GFP-tagged *Plp* for myelin proteolipid protein in retrosplenial dysgranular cortex (***B–C***) and cortical plate (***D–G***) at P15. Scale bars: ***B–C***, 50 μm, ***D–E***, 20 μm and ***F–G***, 5 μm. ***H***, Statistical analysis of the density of *Plp*-GFP$^+$ cells per unit of area (μm^2) at P15. AU, Arbitrary Units. $n \geq 3$; *p* values are shown on the bar graphs. ***I–O***, Gold myelin staining of P15 corpus callosum (***L***, ***M***) and cortex (***N***, ***O***) of control and *Adamts4* knock-out mice. Scale bars: ***J***, 100 μm; ***L***, ***M***, 25 μm; ***N***, 20 μm. ***P***, Statistical analysis of the density of myelin fibers per unit of area (μm^2); $n = 3$; *p* values are shown on the bar graphs.

was further examined in the LPC-injured areas by Gold myelin staining kit, and we observed a marked decrease in the number of newly formed myelin fibers in the *Adamts4* knock-out mice (Fig. 6*H*). Thus, *Adamts4* plays an important role not only in developmental myelination but also in myelin recovery under pathologic conditions.

Discussion

NG2 is a CSPG4 that is highly expressed in migratory and proliferative OPCs (Nishiyama et al., 1991; Levine et al., 1993; Nishiyama et al., 2009; Trotter et al., 2010; Clarke et al., 2012). It is widely used as an OPC marker in both embryonic and adult CNS tissues. As OPCs undergo terminal differentiation, their expression is progressively declined and eventually becomes undetectable in mature myelinating OLs. The significance of this gradual downregulation in differentiating oligodendrocyte and its underlying mechanism has remained elusive.

Previous studies have suggested that the core protein of NG2 contains high-affinity binding sites for PDGF-A (Goretzki et al., 1999), the major *in vivo* mitogen responsible for OPC proliferation (Hart et al., 1989; Pringle et al., 1992). Because OPCs also express PDGFRα, the surface receptor for PDGF-A, it is possible that NG2 proteoglycan serves to enrich PDGF-A on the surface of OPCs, therefore enhancing its binding to PDGFRα and amplifying its downstream signaling event (Nishiyama et al., 1996a,b; Goretzki et al., 1999). This notion is supported by our findings that PDGF-A coimmunoprecipitated with NG2 protein, and coexpression of NG2 can enhance *PDGFR*α-mediated ERK phosphorylation in HEK293T cells (Fig. 3*B*,*C*,*F–H*). Intriguingly, in the CNS tissue, NG2 is also coexpressed with PDGFRβ in capillary endothelial cells (Winkler et al., 2010). It is conceivable that NG2 may carry out a similar function in enriching PDGF-BB on the surface and enhancing PDGFRβ signaling.

What is the possible molecular mechanism underlying the rapid removal of NG2 protein from differentiating OPCs? As PDGFRα signaling promotes OPC proliferation, maintains its

←

callosum; $n \geq 3$. ***T***, Statistical analysis of the number of *Pdgfr*α^+ cells per square millimeter in corpus callosum; $n = 3$. ***U***, ***V***, Representative images showing the double immunofluorescent staining with anti-SOX10 (green) and anti-BrdU (magenta) in primary rat OPC culture treated with or without rhADMATS4 (12 nM) proteinase. SOX10$^+$BrdU$^+$ double-positive cells are represented by arrows. Scale bar, 20 μm. ***W***, Statistical analysis of the BrdU$^+$ cells in SOX10$^+$ oligodendrocytes.

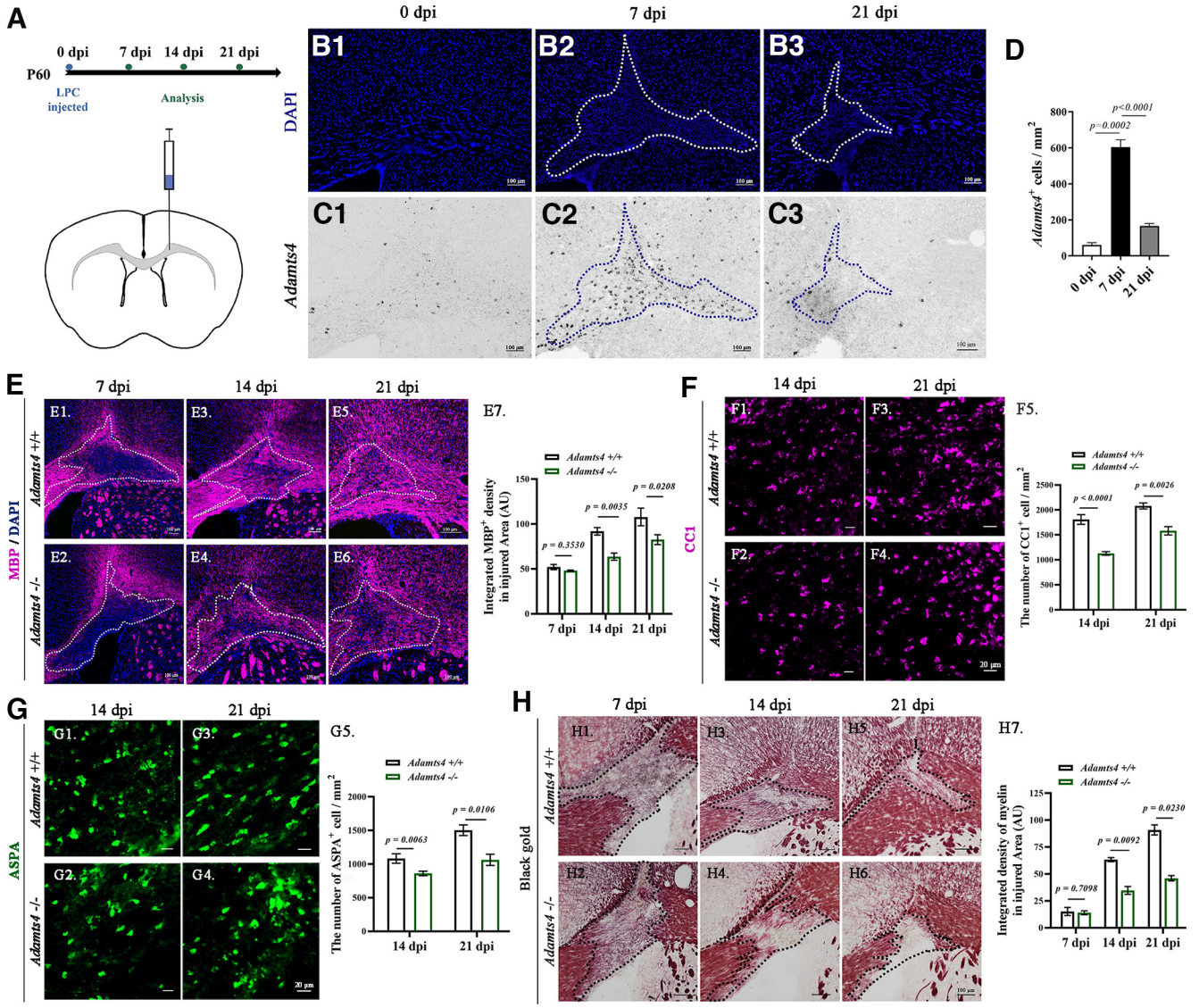

Figure 6. Impaired axonal remyelination in *Adamts4* null mutants. ***A***, Diagram showing LPC-injected site and experimental schedule. ***B1–3***, Injured areas outlined by intense DAPI staining. ***C1–3***, ISH detection of *Adamts4* mRNA expression in adult wild-type mice at 0, 7, and 21 dpi. ***D***, Statistical analysis of the number of *Adamts4*$^+$ cells in injured area (mm^2); $n = 3$. ***E1–7***, Immunofluorescent detection of MBP protein. The lesioned area with dense DAPI signal is outlined by dotted lines. Scale bar, 100 μm. Statistical analysis of the density of MBP immunostaining in injured area (μm^2) at 7, 14, and 21 dpi (***E7***) was presented in ***E7***; $n \geq 3$; p values are shown on the bar graphs. ***F1–G5***, Immunofluorescence staining against anti-CC1 and anti-ASPA of LPC injured *Adamts4*-KO mice corpus collosum at 14 and 21 dpi. Scale bar, 20 μm. Statistical analysis of the number of CC1$^+$ (***F5***) and ASPA$^+$ (***G5***) oligodendrocytes per square millimeter in corpus callosum sections; $n = 3$, $p < 0.05$. ***H1–7***, Gold myelin staining for LPC injured corpus callosum of *Adamts4* knock-out mice at 7, 14, and 21 dpi. Scale bar, 100 μm. Statistical analysis of the myelin density in injured area (μm^2) at 7, 14 and 21 dpi (***H7***); $n = 3$; p values are shown on the bar graphs.

undifferentiated progenitor state, and prevents its premature differentiation (Bögler et al., 1990), expression of PDGFRα and NG2 needs to be downregulated simultaneously during differentiation to facilitate cell cycle exit and achieve full maturation of oligodendrocytes. In this study, we screened the expression of several important members of the ADAMTSs family (*Adamts1*, *Adamts4*, *Adamts5*, *Adamts9*, *Adamts13*, and *Adamts15*) that were reported to be transcribed in the brain (Levy et al., 2015) and found that only *Adamts4* is selectively expressed in oligodendrocytes (Fig. 1*A*,*B*). Double-labeling studies in *Adamts4* heterozygous mice revealed that the increasing *Adamts4* expression in differentiating OPCs was associated with the progressive decline of NG2 immunostaining in the brain white matter between P0 and P10 when OLs undergo active oligodendrocyte differentiation (Fig. 2*A*,*B*). This result slightly differs from a previous report that *Adamts4* is predominantly expressed in mature OLs (Pruvost et al., 2017). In keeping with the findings that *Adamts4* is a well-known proteoglycanase for cleaving CSPGs (Cua et al., 2013; Demircan et al., 2014; Lemarchant et al., 2014; Griffin et al., 2020), we discovered that NG2 protein is likely to be a direct target of ADAMTS4 protease. There are several lines of evidence to support this notion. First, there is an inverse expression relationship between NG2 and ADAMTS4 proteins during postnatal oligodendrocyte differentiation. Second, simultaneous expression of *Adamts4*-Flag and *NG2*-Myc in HEK293T cells produced a shortened 150 kDa NG2 fragment (Fig. 2*E*), and the addition of recombinant human ADAMTS4 protein to the primary OPC culture also increased the production of a proteolytic NG2 fragment (Fig. 2*F*). Third, the shortened isoform of NG2 protein was significantly attenuated in the DIV2 primary culture of *Adamts4* null OPCs (Fig. 2*G*) and in the white matter tissue of *Adamts4* null mutants compared with the controls (Fig. 3*K–M*), indicating that

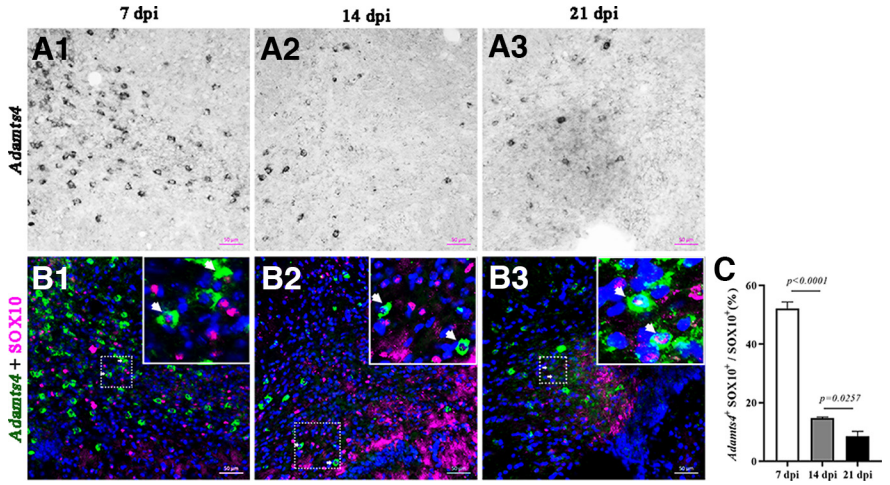

Figure 7. Dynamic expression of *Adamts4* in oligodendrocytes during remyelination. ***A1–3***, Detection of *Adamts4* mRNA expression by ISH from 7 to 21 dpi. Scale bar, 50 µm. ***B1–3***, Tissue slides were subjected to ISH with *Adamts4* riboprobe (green), followed by immunofluorescent staining with SOX10 (magenta). Top right, The magnified view is shown in the white box, and *Adamts4*$^{+}$ *Sox10*$^{+}$ cells are represented by white arrows. Scale bar, 50 µm. ***C***, Statistical analysis of the percentage of *Adamts4* $^{+}$ cells in SOX10^{+} oligodendrocytes in injured area; $n \geq 3$.

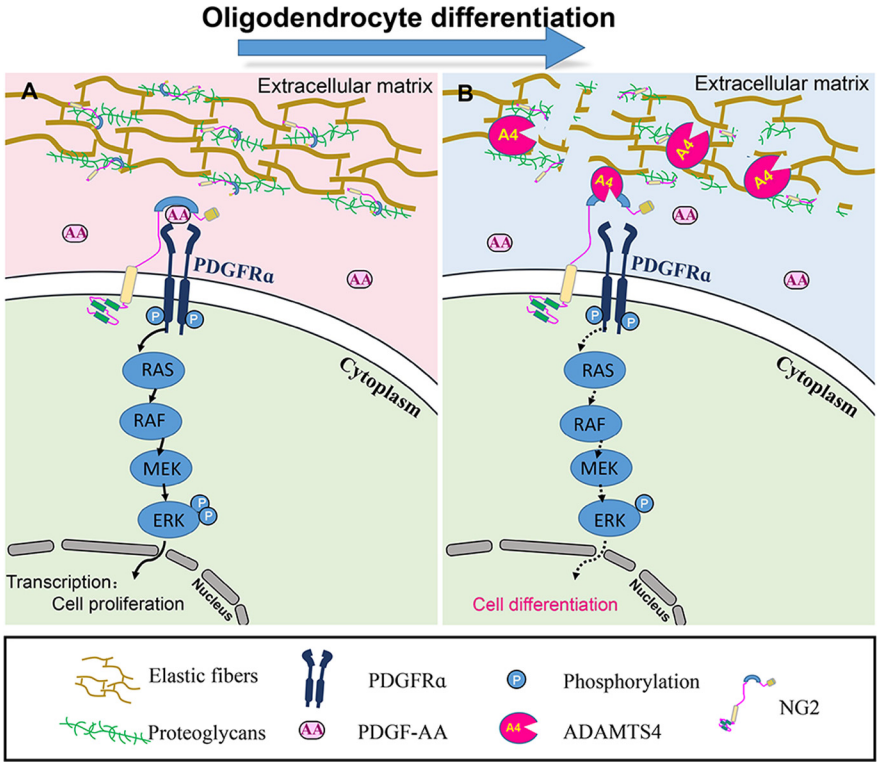

Figure 8. Model for ADAMTS4 function in NG2 cleavage and enhancement of oligodendrocyte differentiation. ***A***, In the absence of ADAMTS4, NG2 enriches PDGF-A on the OPCs surface and enhances its binding and activation of PDGFRα signaling pathway (ERK phosphorylation) that inhibits OL differentiation. ***B***, Extracellular ADAMTS4 cleaves the NG2 protein and reduces the binding of the extracellular growth factor PDGFAA to the receptor PDGFRα and subsequent ERK phosphorylation, facilitating OL differentiation and myelination.

disruption of *Adamts4* impeded the cleavage of NG2 protein in mutant mice and likely contributes to the removal of NG2 surface protein during OL differentiation process. Consistent with this idea, we found that coexpression of NG2 with PDGFRα in HEK293T cells indeed significantly increased its activation and ERK phosphorylation (Fig. 3*F*,*H*). However, when cells were treated with ADAMTS4 conditional medium or recombinant ADAMTS4 protein, NG2 was cleaved and lost its ability to enhance PDGFRα activation, leading to a significant reduction of ERK phosphorylation (Fig. 3*F–J*). In analogy, in the developing CNS, the release of *Adamts4* from differentiating OPCs could digest NG2 protein on the surface and mitigate PDGFRα signaling, leading to slower cell division and accelerated terminal differentiation (Fig. 8).

Because PDGFRα and NG2 are involved in OPC proliferation and differentiation (Sun et al., 2017), it is not surprising to find that *Adamts4* modulates OL differentiation and early myelin development. In the *Adamts4*$^{-/-}$; *Plp*-eGFP mice, expression of GFP in early postnatal brain tissues (P15–P30) was significantly reduced (Fig. 4*A*,*C*,*D*,*K*). Similarly, the number of CC1^{+} and ASPA^{+} mature OLs also decreased in the corpus callosum of *Adamts4*$^{-/-}$ mice (Fig. 4*E–H*,*L*,*M*). Meanwhile, the slightly increased number of undifferentiated *Pdgfr*α^{+} OPCs was noticed in the corpus callosum of *Adamts4* mutant at P15 (Fig. 4*O–T*), possibly because of a compensatory mechanism as a result of slowed cell differentiation. In fact, *Adamts4* is only upregulated during the differentiation stage, presumably after the OPC population has reached a steady state without significant cell division as the steady state of OPCs is primarily determined by the limited supply of endogenous PDGFA (Fig. 4*O–W*). It is more likely that downregulation of PDGFA signaling as a result of *Adamts4* upregulation would not significantly affect cell division and the activation of phosphatidylinositol 3-kinase and the Akt pathway at this stage (Fig. 3*K*,*O*). Instead, it can have a higher impact on cell differentiation and thus Erk phosphorylation (Fig. 3). Therefore, disruption of *Adamts4* expression in the oligodendrocyte lineage has a chief effect on its timely differentiation and maturation, consistent with its selective expression in differentiating OPCs or NFOs. In addition, GFP-tagged *Plp* and Gold myelin staining revealed fewer and shorter processes that are elaborated by oligodendrocytes in the cortical plate of P15 *Adamts4*$^{-/-}$ mice (Fig. 5). Based on these and other observations, we propose that during OL differentiation stage, the release of ADAMTS4 from differentiating OPCs and NFOs serves to cleave the NG2 core protein, abolishing its ability to enrich PDGF-A and therefore reducing its binding to PDGFRα. The diminished NG2 surface protein and PDGFRα signaling can further facilitate the terminal differentiation of OPCs, providing a forward-feeding regulation for oligodendrocyte maturation (Fig. 8). However, additional studies are needed

to provide the direct evidence that NG2 cleavage is necessary for the timely differentiation of oligodendrocytes instead of a parallel occurrence. Conceivably, a ADAMTS4-resistant NG2 molecule could be transfected into OPCs and then examine whether it can delay oligodendrocyte differentiation. Unfortunately, it is difficult to obtain the ADAMTS4-resistant NG2 molecule because we do not know the exact cleavage site and sequence of the NG2 protein.

It is well documented that adult OPCs are capable of differentiating into mature oligodendrocytes during the remyelination stage in the lesioned CNS. Many factors are involved in this process that might affect the biological activity of oligodendrocytes and their ability to form new myelin sheaths. Increasing evidence suggests that the CSPGs and other extracellular matrix molecules are upregulated in the injured CNS and contribute to the formation of glial scar (Asher et al., 2000, 2002; Davies et al., 2004; Beggah et al., 2005; Keough et al., 2016). Moreover, CSPGs are known to inhibit oligodendroglial process outgrowth (Davies et al., 2004; Galtrey and Fawcett, 2007; Fitch and Silver, 2008; Siebert and Osterhout, 2011), and inhibition of CSPGs synthesis and deposition was shown to enhance myelination and regeneration *in vivo* (Lau et al., 2012; Keough et al., 2016). In keeping with these observations, we demonstrated that ADAMTS4 can cleave CSPG4/NG2 and enhance myelin repair after injury. In the LPC-induced demyelinating area, the expression of *Adamts4* mRNA in differentiating and mature OLs increased dramatically and therefore can help to remove NG2 protein to enhance cell differentiation and process outgrowth (Fig. 6*C*,*D*). In *Adamts4* null mice, the lessened removal of NG2 and slower extinction of PDGFRα signaling would eventually hinder the remyelinating process. In support of this idea, we found $CC1^+$, $ASPA^+$, and MBP^+ OLs were decreased significantly in injured areas of *Adamts4* null mice at 14 and 21 dpi (Fig. 6*E*–*G*). The positive effect of *Adamts4* on NG^{2+} OPC differentiation in response to myelin injury in adult tissue is consistent with its role in enhancing OPC maturation during development. Therefore, *Adamts4* possesses an important role in myelin development and repair, making it a potential therapeutic target for the treatment of demyelinating diseases.

References

Asher RA, Morgenstern DA, Fidler PS, Adcock KH, Oohira A, Braistead JE, Levine JM, Margolis RU, Rogers JH, Fawcett JW (2000) Neurocan is upregulated in injured brain and in cytokine-treated astrocytes. J Neurosci 20:2427–2438.

Asher RA, Morgenstern DA, Shearer MC, Adcock KH, Pesheva P, Fawcett JW (2002) Versican is upregulated in CNS injury and is a product of oligodendrocyte lineage cells. J Neurosci 22:2225–2236.

Beggah AT, Dours-Zimmermann MT, Barras FM, Brosius A, Zimmermann DR, Zurn AD (2005) Lesion-induced differential expression and cell association of Neurocan, Brevican, Versican V1 and V2 in the mouse dorsal root entry zone. Neuroscience 133:749–762.

Bhakoo KK, Craig TJ, Styles P (2001) Developmental and regional distribution of aspartoacylase in rat brain tissue. J Neurochem 79:211–220.

Bögler O, Wren D, Barnett SC, Land H, Noble M (1990) Cooperation between two growth factors promotes extended self-renewal and inhibits differentiation of oligodendrocyte-type-2 astrocyte (O-2A) progenitor cells. Proc Natl Acad Sci U S A 87:6368–6372.

Chen Y, Mei R, Teng P, Yang A, Hu X, Zhang Z, Qiu M, Zhao X (2015) TAPP1 inhibits the differentiation of oligodendrocyte precursor cells via suppressing the Mek/Erk pathway. Neurosci Bull 31:517–526.

Clarke LE, Young KM, Hamilton NB, Li H, Richardson WD, Attwell D (2012) Properties and fate of oligodendrocyte progenitor cells in the corpus callosum, motor cortex, and piriform cortex of the mouse. J Neurosci 32:8173–8185.

Cua RC, Lau LW, Keough MB, Midha R, Apte SS, Yong VW (2013) Overcoming neurite-inhibitory chondroitin sulfate proteoglycans in the astrocyte matrix. Glia 61:972–984.

Davies JE, Tang X, Denning JW, Archibald SJ, Davies SJ (2004) Decorin suppresses neurocan, brevican, phosphacan and NG2 expression and promotes axon growth across adult rat spinal cord injuries. Eur J Neurosci 19:1226–1242.

Demircan K, Topcu V, Takigawa T, Akyol S, Yonezawa T, Ozturk G, Ugurcu V, Hasgul R, Yigitoglu MR, Akyol O, McCulloch DR, Hirohata S (2014) ADAMTS4 and ADAMTS5 knockout mice are protected from versican but not aggrecan or brevican proteolysis during spinal cord injury. Biomed Res Int 2014:693746.

Fitch MT, Silver J (2008) CNS injury, glial scars, and inflammation: inhibitory extracellular matrices and regeneration failure. Exp Neurol 209:294–301.

Galtrey CM, Fawcett JW (2007) The role of chondroitin sulfate proteoglycans in regeneration and plasticity in the central nervous system. Brain Res Rev 54:1–18.

Goretzki L, Burg MA, Grako KA, Stallcup WB (1999) High-affinity binding of basic fibroblast growth factor and platelet-derived growth factor-AA to the core protein of the NG2 proteoglycan. J Biol Chem 274:16831–16837.

Griffin JM, Fackelmeier B, Clemett CA, Fong DM, Mouravlev A, Young D, O'Carroll SJ (2020) Astrocyte-selective AAV-ADAMTS4 gene therapy combined with hindlimb rehabilitation promotes functional recovery after spinal cord injury. Exp Neurol 327:113232.

Hart IK, Richardson WD, Bolsover SR, Raff MC (1989) PDGF and intracellular signaling in the timing of oligodendrocyte differentiation. J Cell Biol 109:3411–3417.

Huang H, Teng P, Mei R, Yang A, Zhang Z, Zhao X, Qiu M (2017) Tmeff2 is expressed in differentiating oligodendrocytes but dispensable for their differentiation *in vivo*. Sci Rep 7:337.

Huang H, He W, Tang T, Qiu M (2023) Immunological markers for central nervous system glia. Neurosci Bull 39:379–392.

Jiang C, Yang W, Fan Z, Teng P, Mei R, Yang J, Yang A, Qiu M, Zhao X (2018) AATYK is a novel regulator of oligodendrocyte differentiation and myelination. Neurosci Bull 34:527–533.

Keough MB, Rogers JA, Zhang P, Jensen SK, Stephenson EL, Chen T, Hurlbert MG, Lau LW, Rawji KS, Plemel JR, Koch M, Ling C-C, Yong VW (2016) An inhibitor of chondroitin sulfate proteoglycan synthesis promotes central nervous system remyelination. Nat Commun 7:11312.

Kuboyama K, Tanga N, Suzuki R, Fujikawa A, Noda M (2017) Protamine neutralizes chondroitin sulfate proteoglycan-mediated inhibition of oligodendrocyte differentiation. PLoS One 12:e0189164.

Kucharova K, Stallcup WB (2010) The NG2 proteoglycan promotes oligodendrocyte progenitor proliferation and developmental myelination. Neuroscience 166:185–194.

Larsen PH, Wells JE, Stallcup WB, Opdenakker G, Yong VW (2003) Matrix metalloproteinase-9 facilitates remyelination in part by processing the inhibitory NG2 proteoglycan. J Neurosci 23:11127–11135.

Lau LW, Keough MB, Haylock-Jacobs S, Cua R, Döring A, Sloka S, Stirling DP, Rivest S, Yong VW (2012) Chondroitin sulfate proteoglycans in demyelinated lesions impair remyelination. Ann Neurol 72:419–432.

Lemarchant S, Pruvost M, Montaner J, Emery E, Vivien D, Kanninen K, Koistinaho J (2013) ADAMTS proteoglycanases in the physiological and pathological central nervous system. J Neuroinflammation 10:133.

Lemarchant S, Pruvost M, Hébert M, Gauberti M, Hommet Y, Briens A, Maubert E, Gueye Y, Féron F, Petite D, Mersel M, do Rego J-C, Vaudry H, Koistinaho J, Ali C, Agin V, Emery E, Vivien D (2014) tPA promotes ADAMTS-4-induced CSPG degradation, thereby enhancing neuroplasticity following spinal cord injury. Neurobiol Dis 66:28–42.

Levine JM, Stincone F, Lee YS (1993) Development and differentiation of glial precursor cells in the rat cerebellum. Glia 7:307–321.

Levy C, Brooks JM, Chen J, Su J, Fox MA (2015) Cell-specific and developmental expression of lectican-cleaving proteases in mouse hippocampus and neocortex. J Comp Neurol 523:629–648. PMC]

Mallon BS, Macklin WB (2002) Overexpression of the 3'-untranslated region of myelin proteolipid protein mRNA leads to reduced expression of endogenous proteolipid mRNA. Neurochem Res 27:1349–1360.

Mallon BS, Shick HE, Kidd GJ, Macklin WB (2002) Proteolipid promoter activity distinguishes two populations of NG2-positive cells throughout neonatal cortical development. J Neurosci 22:876–885.

Mattan NS, Ghiani CA, Lloyd M, Matalon R, Bok D, Casaccia P, de Vellis J (2010) Aspartoacylase deficiency affects early postnatal development of oligodendrocytes and myelination. Neurobiol Dis 40:432–443.

Nait-Oumesmar B, Decker L, Lachapelle F, Avellana-Adalid V, Bachelin C, Baron-Van Evercooren A (1999) Progenitor cells of the adult mouse subventricular zone proliferate, migrate and differentiate into oligodendrocytes after demyelination. Eur J Neurosci 11:4357–4366.

Nishiyama A, Dahlin KJ, Prince JT, Johnstone SR, Stallcup WB (1991) The primary structure of NG2, a novel membrane-spanning proteoglycan. J Cell Biol 114:359–371.

Nishiyama A, Lin XH, Giese N, Heldin CH, Stallcup WB (1996a) Co-localization of NG2 proteoglycan and PDGF alpha-receptor on O2A progenitor cells in the developing rat brain. J Neurosci Res 43:299–314.

Nishiyama A, Lin XH, Giese N, Heldin CH, Stallcup WB (1996b) Interaction between NG2 proteoglycan and PDGF alpha-receptor on O2A progenitor cells is required for optimal response to PDGF. J Neurosci Res 43:315–330.

Nishiyama A, Komitova M, Suzuki R, Zhu X (2009) Polydendrocytes (NG2 cells): multifunctional cells with lineage plasticity. Nat Rev Neurosci 10:9–22.

Pringle NP, Mudhar HS, Collarini EJ, Richardson WD (1992) PDGF receptors in the rat CNS: during late neurogenesis, PDGF alpha-receptor expression appears to be restricted to glial cells of the oligodendrocyte lineage. Development 115:535–551.

Pruvost M, Lépine M, Leonetti C, Etard O, Naveau M, Agin V, Docagne F, Maubert E, Ali C, Emery E, Vivien D (2017) ADAMTS-4 in oligodendrocytes contributes to myelination with an impact on motor function. Glia 65:1961–1975.

Qi Y, Cai J, Wu Y, Wu R, Lee J, Fu H, Rao M, Sussel L, Rubenstein J, Qiu M (2001) Control of oligodendrocyte differentiation by the Nkx2.2 homeodomain transcription factor. Development 128:2723–2733.

Siebert JR, Osterhout DJ (2011) The inhibitory effects of chondroitin sulfate proteoglycans on oligodendrocytes. J Neurochem 119:176–188.

Sun Y, Deng Y, Xiao M, Hu L, Li Z, Chen C (2017) Chondroitin sulfate proteoglycans inhibit the migration and differentiation of oligodendrocyte precursor cells and its counteractive interaction with laminin. Int J Mol Med 40:1657–1668.

Tortorella MD, et al. (1999) Purification and cloning of aggrecanase-1: a member of the ADAMTS family of proteins. Science 284:1664–1666.

Tripathi RB, Clarke LE, Burzomato V, Kessaris N, Anderson PN, Attwell D, Richardson WD (2011) Dorsally and ventrally derived oligodendrocytes have similar electrical properties but myelinate preferred tracts. J Neurosci 31:6809–6819.

Trotter J, Karram K, Nishiyama A (2010) NG2 cells: properties, progeny and origin. Brain Res Rev 63:72–82.

Winkler EA, Bell RD, Zlokovic BV (2010) Pericyte-specific expression of PDGF beta receptor in mouse models with normal and deficient PDGF beta receptor signaling. Mol Neurodegener 5:32.

Zhang C, Huang H, Chen Z, Zhang Z, Lu W, Qiu M (2020) The transcription factor NKX2-2 regulates oligodendrocyte differentiation through domain-specific interactions with transcriptional corepressors. J Biol Chem 295:1879–1888.

Zhu Q, Zhao X, Zheng K, Li H, Huang H, Zhang Z, Mastracci T, Wegner M, Chen Y, Sussel L, Qiu M (2014) Genetic evidence that Nkx2.2 and Pdgfra are major determinants of the timing of oligodendrocyte differentiation in the developing CNS. Development 141:548–555.

Zhu Y, Li H, Li K, Zhao X, An T, Hu X, Park J, Huang H, Bin Y, Qiang B, Yuan J, Peng X, Qiu M (2013) Necl-4/SynCAM-4 is expressed in myelinating oligodendrocytes but not required for axonal myelination. PLoS One 8:e64264.